



HAL
open science

Atomic data from the IRON project. LXVII. Electron impact excitation of Fe XIII

P. J. Storey, C. J. Zeippen

► **To cite this version:**

P. J. Storey, C. J. Zeippen. Atomic data from the IRON project. LXVII. Electron impact excitation of Fe XIII. *Astronomy and Astrophysics - A&A*, 2010, 511, 10.1051/0004-6361/200912689. insu-03625651

HAL Id: insu-03625651

<https://insu.hal.science/insu-03625651>

Submitted on 31 Mar 2022

HAL is a multi-disciplinary open access archive for the deposit and dissemination of scientific research documents, whether they are published or not. The documents may come from teaching and research institutions in France or abroad, or from public or private research centers.

L'archive ouverte pluridisciplinaire **HAL**, est destinée au dépôt et à la diffusion de documents scientifiques de niveau recherche, publiés ou non, émanant des établissements d'enseignement et de recherche français ou étrangers, des laboratoires publics ou privés.



Distributed under a Creative Commons Attribution 4.0 International License

Atomic data from the IRON project

LXVII. Electron impact excitation of Fe XIII[★]

P. J. Storey¹ and C. J. Zeippen²

¹ Department of Physics and Astronomy, University College London, Gower Street, London WC1E 6BT, UK
e-mail: pjs@star.ucl.ac.uk

² Observatoire de Paris, UMS 2201, CNRS/INSU, 61 avenue de l'Observatoire, 75014 Paris, France

Received 12 June 2009 / Accepted 14 December 2009

ABSTRACT

A new *R*-matrix calculation of rate coefficients for electron collisional excitation of Fe XIII is presented and compared to recent calculations of comparable complexity. At temperatures at which Fe¹²⁺ is typically found in the solar corona, the present results, which use the intermediate coupling frame transformation method, show significant differences compared to some earlier work. We use a large configuration interaction calculation with extensive correlation to assess the accuracy of our and earlier workers' scattering targets.

Key words. atomic data – Sun: corona – techniques: spectroscopic

1. Introduction

The rates for electron impact excitation of Fe¹²⁺ are principally of interest for collisionally ionized gases such as the corone of the Sun and other stars and fusion plasmas. In such conditions Fe¹²⁺ has its maximum abundance at an electron temperature of $\approx 1.6 \times 10^6$ K (Bryans et al. 2006). At this temperature electron collisions can excite the levels of the ground $3s^23p^2$ configuration and also the higher lying $3s3p^3$ and $3s^23p3d$ configurations. Radiative decays from these two latter configurations give rise to spectral lines in the EUV at wavelengths between 200 and 500 Å, while transitions within the ground configuration result in visible and UV lines. The relative intensities of these lines provide many useful temperature and density diagnostics as discussed, for example, by Keenan et al. (1995) or Landi (2002) and references therein.

Cross-sections for electron collisional excitation of the terms of the $3s^23p^2$ configuration were first calculated by Czyzak et al. (1967) in the distorted wave approximation, while Flower (1971) used the same method and included the additional configurations, $3s3p^3$ and $3s^23p3d$. These early scattering calculations, limited by available computing resources, both in hardware and software, were unable to incorporate the significant configuration interaction in this ion, which was discussed by Flower & Nussbaumer (1974) in some detail. The distorted wave method was also used by Fawcett & Mason (1989), who used a limited configuration basis and the distorted wave method but used Slater parameter optimization to bring the target energies into better agreement with experiment. As we shall see in later sections of this paper, the omission of important configuration interaction leads to significant errors in oscillator and collision strengths and is still an issue with some of the most recent

calculations. The early calculations employing the distorted wave approximation could only approximate the effects of resonances. The most recent work (Tayal 1995; Gupta & Tayal 1998; Tayal 2000; Aggarwal & Keenan 2004, 2005) and the present work employ the close-coupling approximation to delineate resonance structures in detail. The calculations described in the first three of these papers, and the present one, also account for relativistic effects through the use of the Breit-Pauli Hamiltonian, while Aggarwal & Keenan (2004, 2005) use a fully relativistic treatment. The calculation described in the following sections uses the *R*-matrix formulation of the close-coupling approximation combined with the intermediate coupling frame transformation method. Details and references for these techniques follow in Sect. 2.2

2. Atomic data

2.1. Background

In Fig. 1 we show the distribution of the energetically lowest electron configurations of Fe¹²⁺. Transitions between the $3s3p^3$ and $3s^23p3d$ configurations and the ground $3s^23p^2$ give rise to the observed spectral lines in the far UV.

In selecting a set of configurations to form the scattering target, two considerations need to be borne in mind:

Firstly, levels of the $3s3p^3$ and $3s^23p3d$ configurations may be populated by cascade from levels of energetically higher configurations. For this process to be effective, there should be strong electric dipole transitions between the higher configurations and $3s3p^3$ and $3s^23p3d$. In Fe¹²⁺, the relevant configurations in the $n = 3$ complex are $3p^4$, $3s3p^23d$ and $3s^23d^2$. These three configurations can be populated by electron excitation from the ground configuration, although the process is expected to be relatively weak as they are of the same parity as the ground configuration. The process of population by excitation and radiative cascade may, nonetheless, be significant for those

* Full Tables 7 and 8 are only available in full in electronic form at the CDS via anonymous ftp to cdsarc.u-strasbg.fr (130.79.128.5) or via <http://cdsweb.u-strasbg.fr/cgi-bin/qcat?J/A+A/511/A78>

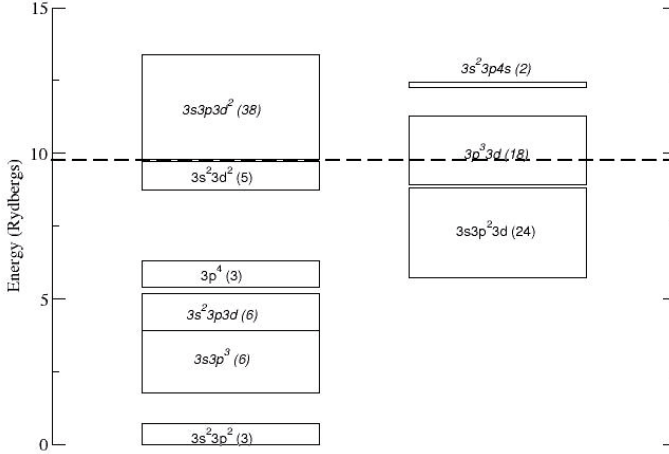


Fig. 1. The energetically lowest electron configurations of Fe^{12+} . Numbers in parentheses indicate the number of terms in that configuration. Odd parity configurations are indicated by italics. The dashed line indicates the extent of the 54 terms in the close-coupling expansion.

states of $3s3p^3$ and $3s^23p3d$ for which direct electron excitation from the ground terms is inefficient.

Secondly, those configurations which are connected to $3s3p^3$ and $3s^23p3d$ by strong electric dipole transitions are also those to which important resonance series converge and these resonances may have a significant effect on collision cross-sections *between* levels of the $3s3p^3$ and $3s^23p3d$ configurations.

For these two reasons it is important that all levels of the $3p^4$, $3s3p^23d$ and $3s^23d^2$ configurations are included in the close coupling expansion for the scattering process. The dashed line in Fig. 1 shows the extent of the target in our calculation, which comprises 54 *LS* terms and 114 levels. Other configurations of the $n = 3$ complex are included in the expansion of the target wavefunctions and these are discussed further in the next section.

2.2. The scattering target

The strongest Fe XIII UV emission lines are excited by electron collisional transitions from the levels of the ground electron configuration, principally the $3s^23p^2\ ^3P_J$ levels. We seek a representation of the scattering target where the strongest of these collisional excitation processes are accurately treated. To this end, we construct a large multi-configuration basis incorporating correlation orbitals, with the aim of determining accurate values for the electric dipole oscillator strengths between the levels of the $3s^23p^2$ configuration and the upper levels responsible for the UV emission lines. The results of this large 72 configuration (hereafter 72CF) calculation can be compared with those from our, and other workers target calculations to obtain an estimate of the quality of the resulting collision strengths, at least for the strong dipole transitions.

In Table 1, we list the electron configurations in the 72CF calculation. The wave functions were calculated with the general purpose atomic structure code SUPERSTRUCTURE (Eissner et al. 1974; Nussbaumer & Storey 1978), and the scaling parameters, λ_{nl} , for the statistical model potentials in which the orbital functions are calculated are given in Table 2. A negative scaling parameter signifies a correlation orbital that is calculated in a Coulomb potential with central charge number $Z/|\lambda_{nl}|$ where $Z = 26$. Table 3 shows the resulting *gf* values between the terms of the three energetically lowest configurations calculated in *LS*-coupling in the length and velocity formulations, which

Table 1. Electron configuration basis for the 72CF calculation.

$3s^2 3p^2$	$3s 3p^3$
$3p^4$	
$3s 3p^2 3d$	$3s^2 3p 3d$
	$3p^3 3d$
$3s^2 3d^2$	$3s 3p 3d^2$
$3p^2 3d^2$	
$3s 3d^3$	$3p 3d^3$
$3s^2 3p \bar{4}l$	$3s 3p^2 \bar{4}l$
$3p^3 \bar{4}l$	$3s^2 3d \bar{4}l$
$3s 3p 3d \bar{4}l$	$l = 0, 1, 2, 3$
$3s^2 3p \bar{5}l$	$3s 3p^2 \bar{5}l$
$3p^3 \bar{5}l$	$3s^2 3d \bar{5}l$
$3s 3p 3d \bar{5}l$	$l = 0, 1, 2, 3, 4$
$3s^2 \bar{4}l^2$	$3s 3p \bar{4}l^2$
$3p^2 \bar{4}l^2$	$3p 3d \bar{4}l^2$
	$l = 0, 1, 2, 3$

Table 2. Orbital scaling parameters[†] for the 72CF calculation.

1s	1.4009	2p	1.0577
3s	1.1331	3p	1.1056
$\bar{4}s$	-0.9817	$\bar{4}p$	-0.9335
$\bar{5}s$	-1.2067	$\bar{5}p$	-1.1951
		$\bar{3}d$	1.1310
		$\bar{4}d$	-0.9132
		$\bar{4}f$	-0.8931
		$\bar{5}d$	1.0955
		$\bar{5}f$	-1.5571
		$\bar{5}g$	-1.2925

Notes. ([†]) See text for physical significance of the scaling parameters.

show good agreement. Also shown in Table 3 are the *gf* values obtained in the length formulation using the configuration basis from Table 4. This configuration basis, which will be used to describe the target for the scattering calculation, contains only configurations from the $n = 3$ complex with a maximum of three electrons in the 3d shell. The average absolute difference in the length *gf* values between the target and 72CF calculations is 2.5%. We also tabulate the results of a calculation by Young (2004) which uses configurations from the $n = 3$ complex plus a limited set of configurations involving $n = 4$ orbitals. For this calculation, the average absolute difference from our 72CF results is 1.2%.

The target configuration basis described in Table 4 gives *gf* values in good agreement with the 72CF calculation but has none of the disadvantages of a target including correlation orbitals which can lead to physically unrealistic resonances. The configuration basis of Young (2004) gives slightly superior *gf* values without using correlation $n = 4$ orbitals but such physical $n = 4$ orbitals cause the *R*-matrix boundary to be significantly larger which greatly increases the computational cost of the scattering calculation.

We now compare the results of our 72CF and target calculations with those from the two most recently published Fe^{12+} scattering calculations described by Gupta & Tayal (1998) and Aggarwal & Keenan (2004). Table 5 shows the experimental and calculated level energies for the 27 levels of the three energetically lowest configurations. The 72CF calculation includes one and two-body fine-structure interactions as described in Eissner et al. (1974) whereas our target calculation includes only the one-body spin-orbit interaction for consistency with the *R*-matrix calculation to follow. Two-body fine-structure terms are not yet included in the *R*-matrix codes used in this work. In Table 5 we also give energies obtained after applying the so-called term energy corrections or TEC, (Zeippen et al. 1977; Nussbaumer & Storey 1978) which introduce empirical corrections to the *LS* Hamiltonian matrix to bring the final level energies in to better agreement with experiment.

Gupta & Tayal (1998) used the CIV3 code described by Hibbert (1975) while Aggarwal & Keenan (2004) used the relativistic GRASP code of Dyllal et al. (1989). The mean of the

Table 3. Weighted oscillator strengths, gf , for transitions between terms in Fe¹²⁺.

Transition				72CF (L)	72CF (V)	Young (2004) (L)	Target (L)	
3s ² 3p ²	³ P	–	3s 3p ³	³ D ^o	0.441	0.451	0.442	0.425
		–	3s 3p ³	³ P ^o	0.545	0.563	0.542	0.526
		–	3s 3p ³	³ S ^o	1.749	1.777	1.754	1.774
		–	3s ² 3p 3d	³ P ^o	2.522	2.560	2.570	2.567
		–	3s ² 3p 3d	³ D ^o	6.269	6.356	6.347	6.432
3s ² 3p ²	¹ D	–	3s 3p ³	¹ D ^o	0.467	0.471	0.474	0.477
		–	3s 3p ³	¹ P ^o	0.893	0.917	0.909	0.907
		–	3s ² 3p 3d	¹ D ^o	2.185	2.225	2.193	2.201
		–	3s ² 3p 3d	¹ F ^o	2.885	2.878	2.917	2.940
		–	3s ² 3p 3d	¹ P ^o	0.0004	0.0002		0.0003
3s ² 3p ²	¹ S	–	3s 3p ³	¹ P ^o	0.183	0.185	0.188	0.199
		–	3s ² 3p 3d	¹ P ^o	1.089	1.100	1.099	1.094

Table 4. The target configuration basis and orbital scaling parameters.

Configurations		Scaling parameters [†]	
3s ² 3p ²	3s 3p ³	1s	1.40094
3p ⁴		2s	1.11468
3s 3p ² 3d	3s ² 3p 3d	3s	1.13314
	3p ⁵ 3d	2p	1.05769
3s ² 3d ²	3s 3p 3d ²	3p	1.10557
3p ² 3d ²		3d	1.13097
3s 3d ³	3p 3d ³		

Notes. ^(†) See text for physical significance of the scaling parameters.

absolute differences between theory and experiment is 0.038 Ryd for Gupta & Tayal (1998), 0.209 Ryd for Aggarwal & Keenan (2004), 0.039 Ryd for our target calculation and 0.035 Ryd for our 72CF calculation. On this measure there is little difference in quality between the present target calculation and that of Gupta & Tayal (1998) while the Aggarwal & Keenan (2004) results are significantly less good. Aggarwal & Keenan (2004) explored the significance of increased configuration interaction and showed that a thirteen configuration GRASP calculation gave much better calculated energies than the six configuration calculation that they finally adopted due to computational constraints. The energies resulting from their thirteen configuration calculation are very similar to those of Gupta & Tayal (1998) and the present target, indicating that configuration interaction is the most important consideration here and that using the fully relativistic GRASP code offers no significant advantage over CIV3 and SUPERSTRUCTURE which are based on the Breit-Pauli Hamiltonian.

Although a comparison of calculated energy levels is useful, the quality of the calculated oscillator strengths for the strong dipole allowed transitions from the ground electron configuration to the 3s3p³ and 3s²3p3d configurations is a more meaningful indicator of the accuracy of the corresponding collision strengths. The strong dipole allowed transitions are less affected by resonance effects and, at the electron temperatures where these ions are most abundant in a collisionally ionized medium, the collision strengths have large contributions from high partial waves. The high partial wave contributions are proportional to the absorption oscillator strength for the transition. We therefore compare, in Table 6, the fine-structure absorption oscillator strengths from our 72CF calculation, our target calculation and from the work of Gupta & Tayal (1998) and

Aggarwal & Keenan (2004). In this table the 72CF calculation includes TECs and experimental energies are used where available in the calculation of oscillator strengths from the computed matrix elements.

Considering only those transitions where the 72CF absorption oscillator strength is at least 0.1, we find the average absolute percentage differences from the 72CF results to be 7.1% for our target calculation, 5.9% for Gupta & Tayal (1998) and 26.2% for Aggarwal & Keenan (2004). The results from the present target calculation and from that of Gupta & Tayal (1998) are generally in good agreement with no major differences for any of the stronger transitions. Indeed, the results of Gupta & Tayal (1998) are in slightly better agreement with our 72CF values on average, as might be expected as their basis includes an $n = 4$ correlation orbital, which our target does not. There are, however, significant differences between the results of Aggarwal & Keenan (2004) and the other three calculations for a few transitions. There are particularly large differences for transitions to 3s3p³ ³S₁^o, ¹P₁^o and 3s²3p3d ³P₂, ¹D₂. These discrepancies for pairs of closely lying levels of the same J and parity suggest that the magnitude of the fine-structure interactions between these levels are very different in the work of Aggarwal & Keenan (2004) and the other three calculations described here. To a first approximation, the strength of the fine-structure interaction is inversely proportional to the energy difference between the levels. For the ³S₁^o and ¹P₁^o levels the observed separation is 0.206 Ryd, while Gupta & Tayal (1998) have 0.196 Ryd, our target has 0.213 Ryd and Aggarwal & Keenan (2004) have 0.165 Ryd. Similarly for the ³P₂, ¹D₂ pair, the experimental separation is 0.115 Ryd, Gupta & Tayal (1998) have 0.108 Ryd, our target value is 0.111 Ryd, while Aggarwal & Keenan (2004) find 0.162 Ryd. A test calculation with SUPERSTRUCTURE using the same six configurations as Aggarwal & Keenan (2004) gives energy separations very similar to those reported by them. We conclude that the six configuration basis used by Aggarwal & Keenan (2004) yields energy separations that are significantly different from experiment for these two pairs of levels and that this leads to the oscillator strengths from the ground electron configuration to these levels being inaccurate as shown in Table 6. These differences in the oscillator strengths are reflected in the corresponding collision strengths, as we shall see in the following sections.

2.3. The scattering calculation

The configuration basis describing the target for the present calculation is shown in Table 4. For the scattering calculation the

Table 5. Level energies of the three energetically lowest configurations in Rydberg.

Index	Level	Exp. [†]	72CF (ab initio)	72CF (with TEC)	GT ^a	AK ^b	Target	
1	3s ² 3p ²	³ P ₀	0.	0.	0.	0.	0.	
2		³ P ₁	0.0848	0.0832	0.0836	0.0768	0.0835	0.0808
3		³ P ₂	0.1692	0.1673	0.1672	0.1582	0.1700	0.1657
4		¹ D ₂	0.4380	0.4416	0.4366	0.4366	0.4629	0.4516
5		¹ S ₀	0.8339	0.8436	0.8324	0.8612	0.8497	0.8512
6	3s 3p ³	⁵ S ₀ ^o	1.9558	1.9275	1.9544		1.9719	1.9144
7		³ D ₁ ^o	2.6172	2.6170	2.6164	2.5978	2.7427	2.6099
8		³ D ₂ ^o	2.6186	2.6180	2.6174	2.5982	2.7437	2.6111
9		³ D ₃ ^o	2.6443	2.6423	2.6424	2.6212	2.7683	2.6363
10		³ P ₀ ^o	2.9974	3.0099	2.9973	2.9906	3.1533	2.9968
11		³ P ₁ ^o	3.0045	3.0157	3.0032	2.9956	3.1595	3.0031
12		³ P ₂ ^o	3.0098	3.0205	3.0079	2.9910	3.1649	3.0081
13		¹ D ₂ ^o	3.3025	3.3305	3.3011	3.2968	3.5222	3.3192
14		³ S ₁ ^o	3.7860	3.8575	3.7846	3.8390	4.1498	3.8327
15	3s ² 3p 3d	³ F ₂ ^o	3.9435	3.9621	3.9403	3.9906	4.1285	3.9723
16	3s 3p ³	¹ P ₁ ^o	3.9918	4.0554	3.9903	4.0348	4.3144	4.0452
17	3s ² 3p 3d	³ F ₃ ^o	4.0043	4.0239	4.0023	4.0500	4.1901	4.0338
18		³ F ₄ ^o	4.0880	4.1150	4.0937	4.1366	4.2822	4.1234
19		³ P ₂ ^o	4.4321	4.4985	4.4370	4.4884	4.7668	4.5055
20		³ P ₁ ^o	4.5103	4.5708	4.5124	4.5594	4.8245	4.5794
21		¹ D ₂ ^o	4.5461	4.6116	4.5475	4.5960	4.9284	4.6165
22		³ P ₀ ^o	4.5702	4.6264	4.5722	4.6076	4.8765	4.6295
23		³ D ₁ ^o	4.6156	4.6761	4.6150	4.6642	4.9392	4.6875
24		³ D ₃ ^o	4.6400	4.7051	4.6402	4.6968	4.9694	4.7210
25		³ D ₂ ^o	4.6407	4.7033	4.6407	4.6918	4.9689	4.7162
26		¹ F ₃ ^o	5.0746	5.1565	5.0731	5.2120	5.4286	5.1790
27		¹ P ₁ ^o	5.2006	5.2901	5.1991	5.2694	5.5975	5.3016

Notes. ^(†) Jupen et al. (1993); Martin et al. (1995); Penn & Kuhn (1994); ^(a) Gupta & Tayal (1998); ^(b) Aggarwal & Keenan (2004).

lowest 54 *LS* terms are included which give rise to 114 levels. As stated above the target includes all states belonging to the five energetically lowest electron configurations plus all levels of the 3s²3d² configuration and 17 levels of the 3p³3d configuration.

Ideally, the whole 3p³3d configuration would be included. In practice, including the whole configuration would also involve including most of a further configuration (3s3p3d², see Fig. 1), significantly enlarging the size of the scattering problem.

The *R*-matrix method used in this calculation is described elsewhere (Hummer et al. 1993, and references therein). As outlined above, we include mass and Darwin relativistic energy shifts, but not the one- and two-body fine-structure interactions. We use an *R*-matrix boundary radius of 2.97 au, to encompass the most extended target orbital (3d). The expansion of each scattered electron partial wave is over a basis of 20 functions within the *R*-matrix boundary, and the partial wave expansion extends to a maximum total orbital angular momentum quantum number of $L = 18$. The outer region calculation is carried out using the intermediate-coupling frame transformation (ICFT) method described by Griffin et al. (1998), in which the transformation to intermediate coupling uses the so-called term-coupling coefficients (TCCs), and is complete up to a total angular momentum quantum number, $J = 31/2$. We note that with the ICFT method, TCCs can be combined with experimental fine structure energies to generate collision strengths that map the resonance structures between the levels of a term. Collision strengths were calculated at a total of 16 000 energies in the region where some channels are closed with an energy spacing

of 0.00061 Ryd. We have supplemented this calculation, which includes exchange, with a non-exchange calculation that extends from $J = 33/2$ to $J = 101/2$. Dipole-allowed transitions are also topped-up to infinite partial wave using an intermediate coupling version of the Coulomb-Bethe method as described by Burgess (1974) while non-dipole allowed transitions are topped-up assuming that the collision strengths form a geometric progression in J for $J > 50$. Once all collision strengths have been corrected for missing angular momenta, they are extrapolated to energies higher than 100 Ryd using techniques and asymptotic expressions discussed by Burgess & Tully (1992).

3. Comparisons

3.1. Collision strengths

In this section we compare our calculated collision strengths with those of the two other recent scattering calculations of comparable complexity by Gupta & Tayal (1998) and Aggarwal & Keenan (2004). In Fig. 2 we plot our results against those of Gupta & Tayal (1998) calculated at 15 Ryd. All the collision strengths between the three energetically lowest levels and all levels of the 3s3p³ and 3s²3p3d configurations are shown. The agreement is excellent, particularly for the stronger transitions. By contrast, the comparison with the results of Aggarwal & Keenan (2004), shown in Fig. 3, shows several large differences. The transitions are labelled by their level indices.

Transitions to levels 14 and 16 (3s3p³ ³S₁^o and ¹P₁^o), show large differences while there are also significant differences for

Table 6. Absorption oscillator strengths for transitions between the levels of the ground configuration, $3s^2 3p^2$ and the configurations $3s 3p^3$ and $3s^2 3p 3d$.

Upper level	Lower level					
	3P_0	3P_1	3P_2	1D_2	1S_0	
$3s 3p^3$	$^3D_1^o$	0.0744 ^a	0.0069	0.00016	0.00045	0.00031
		0.0717 ^b	0.0069	0.00014	0.00043	0.00027
		0.069 ^c	0.007	0.0001	0.0004	0.00024
		0.0676 ^d	0.0068	0.00013	0.00039	0.00041
	$^3D_2^o$	0.0505	0.0011	0.00028		
		0.0493	0.0011	0.00027		
		0.048	0.001	0.0002		
		0.0466	0.0011	0.00021		
	$^3D_3^o$			0.0378	0.0035	
				0.0379	0.0030	
				0.037	0.0029	
	$^3P_0^o$		0.0212			
		0.0208				
		0.020				
		0.0209				
$^3P_1^o$	0.0542	0.0291	0.0089	0.00064	0.0018	
	0.0537	0.0280	0.0090	0.00054	0.0017	
	0.053	0.027	0.009	0.0005	0.0015	
	0.0524	0.0262	0.0100	0.00062	0.0016	
$^3P_2^o$		0.0107	0.0534	0.00010		
		0.0113	0.0523	0.00016		
		0.011	0.051	0.0001		
$^1D_2^o$		0.0118	0.0510	0.0		
		0.0016	0.0013	0.0829		
		0.0013	0.0012	0.0884		
$^3S_1^o$		0.001	0.001	0.084		
		0.0012	0.0012	0.0760		
	0.1792	0.1550	0.1912	0.0043	0.0177	
	0.1925	0.1672	0.2001	0.0044	0.0176	
$3s^2 3p 3d$	$^3F_2^o$	0.187	0.163	0.198	0.0056	0.018
		0.1167	0.0956	0.1509	0.0509	0.0432
			0.0016	0.0013	0.0036	
			0.0014	0.0010	0.0033	
$3s 3p^3$	$^1P_1^o$	0.0014	0.0011	0.003		
		0.0013	0.00083	0.0024		
		0.0223	0.0431	0.0055	0.1755	0.1589
		0.0188	0.0407	0.0055	0.1836	0.1815
$3s^2 3p 3d$	$^3F_3^o$	0.025	0.045	0.0076	0.177	0.159
		0.1099	0.1206	0.0576	0.1374	0.0706
				0.0040	0.00030	
				0.0032	0.00027	
$3s 3p^3$	$^3P_2^o$		0.003	0.0002		
			0.0030	0.00032		
		0.1964	0.1238	0.1240		
		0.1973	0.1270	0.1309		
	$^3P_1^o$	0.197	0.126	0.127		
		0.3077	0.1529	0.0317		
		0.8471	0.0017	0.0281	0.0036	0.0014
		0.8369	0.00013	0.0344	0.0033	0.0014
	$^1D_2^o$	0.818	0.0001	0.034	0.0038	0.0010
		0.8184	0.0	0.0372	0.0052	0.0019
			0.2125	0.00057	0.2692	
			0.2049	0.0	0.2859	
$^3P_0^o$		0.195	0.0	0.292		
		0.1361	0.0325	0.3634		
		0.0961				
		0.0998				
	0.098					
	0.1009					

Notes. For each transition, comparison is made between the present 72CF calculation^a, the scattering target^b, the results of Gupta & Tayal (1998)^c and the results of Aggarwal & Keenan (2004)^d.

Table 6. continued.

Upper level	Lower level				
	3P_0	3P_1	3P_2	1D_2	1S_0
$^3D_1^o$	0.1436	0.2455	0.0480	0.0061	0.00031
	0.1972	0.2577	0.0459	0.0051	0.00043
	0.202	0.255	0.045	0.0045	0.0003
	0.2185	0.2599	0.0457	0.0041	0.00028
$^3D_3^o$			0.5635	0.0238	
			0.5943	0.0201	
			0.586	0.022	
$^3D_2^o$			0.6014	0.0205	
		0.2383	0.2094	0.0467	
		0.2738	0.2181	0.0383	
		0.276	0.214	0.038	
$^1F_3^o$		0.2400	0.1928	0.0873	
			0.0248	0.5556	
			0.0211	0.5820	
$^1P_1^o$			0.023	0.573	
			0.0211	0.5849	
	0.0049	0.00070	0.0	0.00041	1.104
	0.0046	0.00072	0.0	0.0	1.134
	0.003	0.0007	0.0	0.0008	1.106
	0.0072	0.00052	0.0	0.0036	1.2380

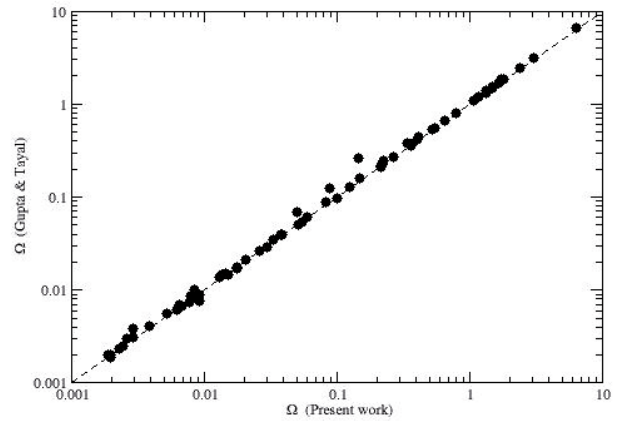


Fig. 2. Comparison of collision strengths at 15 Rydberg from the present work and from Gupta & Tayal (1998). Transitions are included between the three energetically lowest levels and all levels of the $3s 3p^3$ and $3s^2 3p 3d$ configurations.

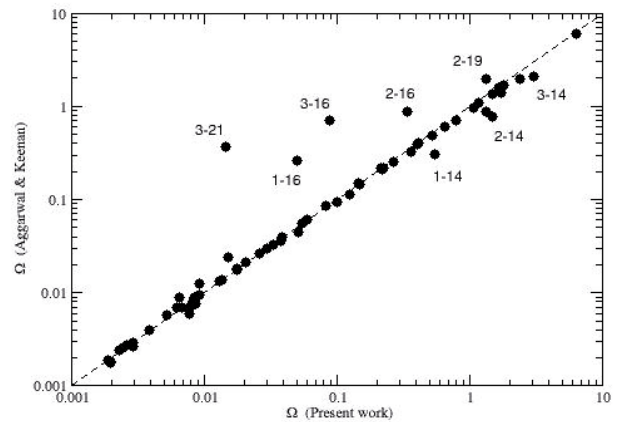


Fig. 3. Comparison of collision strengths at 15 Rydberg from the present work and from Aggarwal & Keenan (2004). Transitions are included between the three energetically lowest levels and all levels of the $3s 3p^3$ and $3s^2 3p 3d$ configurations.

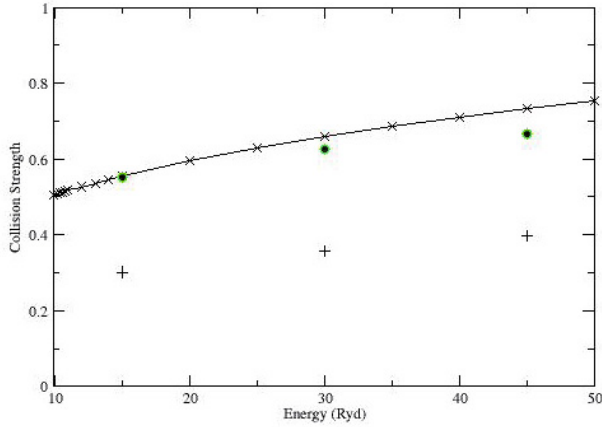


Fig. 4. Comparison of collision strengths for the transition 1–14 in the region of all channels open from the present work (\times), from [Aggarwal & Keenan \(2004\)](#) (+) and from [Gupta & Tayal \(1998\)](#) (filled circles).

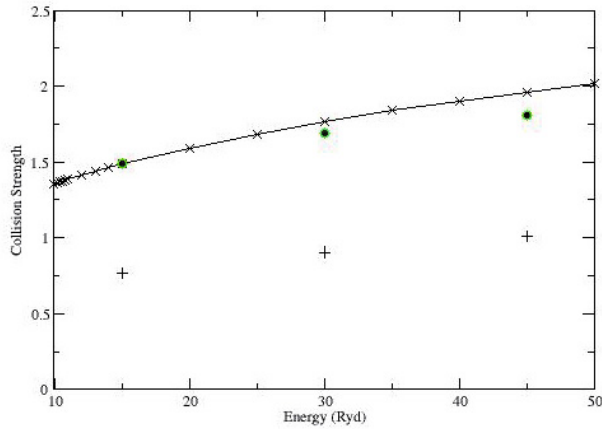


Fig. 5. Comparison of collision strengths for the transition 2–14 in the region of all channels open from the present work (\times), from [Aggarwal & Keenan \(2004\)](#) (+) and from [Gupta & Tayal \(1998\)](#) (filled circles).

transitions to levels 19 and 21 ($3s^23p3d\ ^3P_2^o$ and $^1D_2^o$). These transitions are all optically allowed and are the transitions that were identified as being discrepant in the discussion of oscillator strengths in the previous section. At high electron energies the collision strengths for the optically allowed transitions are dominated by high partial wave contributions whose magnitude is closely related to the absorption oscillator strength for the transition. Figures 4 and 5 show two of the transitions with the largest differences as a function of incident electron energy in the region where all scattering channels are open. These figures confirm that the collision strengths of [Aggarwal & Keenan \(2004\)](#) are, in these two cases, systematically smaller than the present work and that of [Gupta & Tayal \(1998\)](#), which are themselves in good agreement. As discussed in the previous section, we consider that the results of [Aggarwal & Keenan \(2004\)](#) are inaccurate for these transitions due to the limited configuration basis used to expand their target wavefunctions. Although the agreement between the present work and that of [Gupta & Tayal \(1998\)](#) shown in Fig. 2 is very good at 15 Ryd, Figs. 4 and 5 show that, for these two transitions, the two sets of results diverge as the electron energy increases. This effect has already been noted and discussed at length by [Aggarwal & Keenan \(2005\)](#).

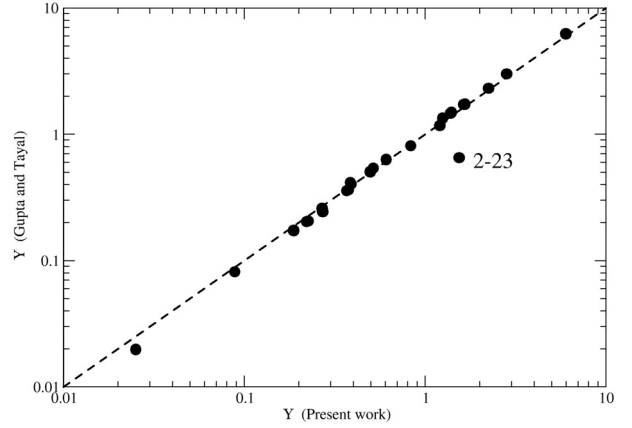


Fig. 6. Comparison of thermally averaged collision strengths at 10^6 K from the present work and from [Gupta & Tayal \(1998\)](#). Transitions are shown between the three energetically lowest levels and all levels of the $3s3p^3$ and $3s^23p3d$ configurations which satisfy the rigorous electric dipole selection rules and also conserve the ionic spin quantum number.

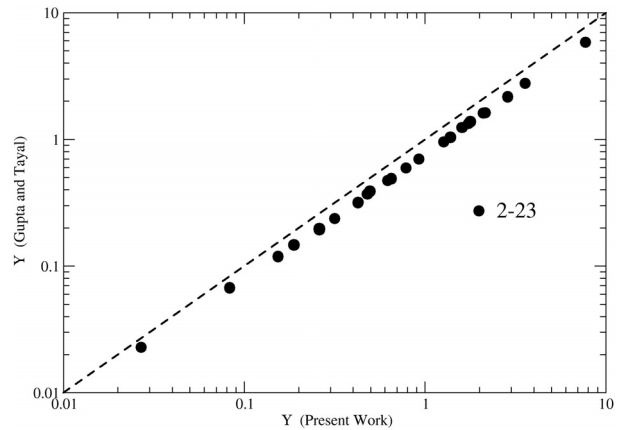


Fig. 7. Comparison of thermally averaged collision strengths at 5×10^6 K from the present work and from [Gupta & Tayal \(1998\)](#). Transitions are included between the three energetically lowest levels and all levels of the $3s3p^3$ and $3s^23p3d$ configurations which satisfy the rigorous electric dipole selection rules and also conserve the ionic spin quantum number.

3.2. Thermally averaged collision strengths

In Table 7 we tabulate thermally averaged collision strengths from the five levels of the ground electron configuration to all levels of the $3s3p^3$ and $3s^23p3d$ configurations at a range of electron temperatures around the temperature of maximum fractional abundance of Fe^{12+} in a collisionally ionized plasma. The complete set of thermally averaged collision strengths for all 114 target levels is available from the CDS (see footnote on front page).

In Figs. 6–8 we compare our results with those of [Gupta & Tayal \(1998\)](#). We begin by comparing thermally averaged collision strengths at 10^6 K for those transitions which correspond to strong optically allowed transitions, in practice those which satisfy the rigorous selection rules and also conserve the spin quantum number of the ion. This comparison is shown in Fig. 6. With the exception of transition 2–23, which appears to be a typographical error in the paper of [Gupta & Tayal \(1998\)](#) the agreement is excellent.

[Aggarwal & Keenan \(2005\)](#) point out that the thermally averaged collision strengths of [Gupta & Tayal \(1998\)](#) are

Table 7. Thermally averaged collision strengths.

<i>i</i>	<i>j</i>	$\log_{10}(T[\text{K}])$							
		5.6	5.8	6.0	6.2	6.4	6.6	6.8	7.0
1	2	5.324(-1) [†]	4.174(-1)	3.097(-1)	2.210(-1)	1.535(-1)	1.048(-1)	7.066(-2)	4.716(-2)
1	3	4.922(-1)	4.018(-1)	3.187(-1)	2.515(-1)	2.015(-1)	1.663(-1)	1.426(-1)	1.270(-1)
1	4	1.977(-1)	1.521(-1)	1.111(-1)	7.827(-2)	5.389(-2)	3.658(-2)	2.462(-2)	1.649(-2)
1	5	6.475(-2)	4.953(-2)	3.568(-2)	2.464(-2)	1.653(-2)	1.088(-2)	7.071(-3)	4.559(-3)
1	6	4.916(-2)	3.796(-2)	2.850(-2)	2.104(-2)	1.534(-2)	1.107(-2)	7.889(-3)	5.543(-3)
1	7	3.843(-1)	3.725(-1)	3.684(-1)	3.735(-1)	3.879(-1)	4.112(-1)	4.420(-1)	4.790(-1)
1	8	8.158(-2)	6.283(-2)	4.692(-2)	3.433(-2)	2.477(-2)	1.767(-2)	1.246(-2)	8.675(-3)
1	9	5.929(-2)	4.316(-2)	3.039(-2)	2.102(-2)	1.450(-2)	1.013(-2)	7.302(-3)	5.519(-3)
1	10	7.236(-3)	5.304(-3)	3.811(-3)	2.710(-3)	1.915(-3)	1.346(-3)	9.388(-4)	6.482(-4)
1	11	2.424(-1)	2.307(-1)	2.257(-1)	2.276(-1)	2.362(-1)	2.507(-1)	2.704(-1)	2.942(-1)
1	12	4.549(-2)	3.327(-2)	2.370(-2)	1.663(-2)	1.156(-2)	7.992(-3)	5.486(-3)	3.736(-3)
1	13	4.196(-2)	3.104(-2)	2.275(-2)	1.660(-2)	1.207(-2)	8.716(-3)	6.223(-3)	4.380(-3)
1	14	4.953(-1)	5.016(-1)	5.165(-1)	5.413(-1)	5.769(-1)	6.235(-1)	6.805(-1)	7.467(-1)
1	15	5.383(-2)	4.107(-2)	3.064(-2)	2.250(-2)	1.633(-2)	1.172(-2)	8.300(-3)	5.795(-3)
1	16	5.789(-2)	5.466(-2)	5.317(-2)	5.336(-2)	5.513(-2)	5.837(-2)	6.288(-2)	6.849(-2)
1	17	4.640(-2)	3.801(-2)	3.167(-2)	2.726(-2)	2.451(-2)	2.309(-2)	2.271(-2)	2.308(-2)
1	18	1.246(-2)	9.446(-3)	7.070(-3)	5.248(-3)	3.864(-3)	2.816(-3)	2.024(-3)	1.431(-3)
1	19	1.854(-2)	1.548(-2)	1.271(-2)	1.024(-2)	8.083(-3)	6.222(-3)	4.667(-3)	3.411(-3)
1	20	1.538(0)	1.588(0)	1.661(0)	1.761(0)	1.893(0)	2.061(0)	2.263(0)	2.498(0)
1	21	8.667(-3)	7.076(-3)	5.605(-3)	4.343(-3)	3.301(-3)	2.461(-3)	1.797(-3)	1.284(-3)
1	22	1.344(-3)	1.101(-3)	8.797(-4)	6.890(-4)	5.290(-4)	3.973(-4)	2.914(-4)	2.086(-4)
1	23	3.630(-1)	3.722(-1)	3.864(-1)	4.073(-1)	4.359(-1)	4.729(-1)	5.180(-1)	5.705(-1)
1	24	1.681(-2)	1.485(-2)	1.299(-2)	1.143(-2)	1.020(-2)	9.302(-3)	8.690(-3)	8.316(-3)
1	25	1.170(-2)	9.508(-3)	7.551(-3)	5.897(-3)	4.534(-3)	3.428(-3)	2.543(-3)	1.850(-3)
1	26	8.860(-3)	7.764(-3)	6.631(-3)	5.527(-3)	4.491(-3)	3.555(-3)	2.743(-3)	2.067(-3)
1	27	1.068(-2)	1.032(-2)	1.008(-2)	1.004(-2)	1.023(-2)	1.065(-2)	1.129(-2)	1.211(-2)
2	3	2.072(0)	1.655(0)	1.265(0)	9.448(-1)	7.037(-1)	5.322(-1)	4.145(-1)	3.355(-1)
2	4	1.342(0)	1.046(0)	7.715(-1)	5.466(-1)	3.777(-1)	2.576(-1)	1.751(-1)	1.196(-1)
2	5	1.374(-1)	1.056(-1)	7.657(-2)	5.332(-2)	3.611(-2)	2.401(-2)	1.576(-2)	1.025(-2)
2	6	1.518(-1)	1.170(-1)	8.834(-2)	6.630(-2)	4.997(-2)	3.815(-2)	2.976(-2)	2.390(-2)
2	7	2.513(-1)	2.151(-1)	1.875(-1)	1.688(-1)	1.580(-1)	1.538(-1)	1.547(-1)	1.594(-1)
2	8	9.035(-1)	8.574(-1)	8.316(-1)	8.299(-1)	8.523(-1)	8.965(-1)	9.593(-1)	1.037(0)
2	9	2.406(-1)	1.781(-1)	1.279(-1)	9.011(-2)	6.301(-2)	4.408(-2)	3.110(-2)	2.231(-2)
2	10	2.765(-1)	2.696(-1)	2.686(-1)	2.743(-1)	2.867(-1)	3.053(-1)	3.293(-1)	3.579(-1)
2	11	4.048(-1)	3.856(-1)	3.765(-1)	3.785(-1)	3.911(-1)	4.133(-1)	4.439(-1)	4.814(-1)
2	12	3.026(-1)	2.551(-1)	2.207(-1)	1.989(-1)	1.883(-1)	1.865(-1)	1.918(-1)	2.022(-1)
2	13	1.585(-1)	1.217(-1)	9.351(-2)	7.273(-2)	5.776(-2)	4.717(-2)	3.983(-2)	3.493(-2)
2	14	1.317(0)	1.337(0)	1.380(0)	1.448(0)	1.544(0)	1.670(0)	1.824(0)	2.003(0)
2	15	1.296(-1)	1.038(-1)	8.387(-2)	6.954(-2)	6.009(-2)	5.458(-2)	5.208(-2)	5.178(-2)
2	16	3.304(-1)	3.265(-1)	3.296(-1)	3.403(-1)	3.588(-1)	3.847(-1)	4.176(-1)	4.567(-1)
2	17	1.136(-1)	8.823(-2)	6.698(-2)	5.021(-2)	3.742(-2)	2.785(-2)	2.079(-2)	1.564(-2)
2	18	9.280(-2)	7.480(-2)	6.082(-2)	5.059(-2)	4.353(-2)	3.903(-2)	3.651(-2)	3.548(-2)
2	19	1.176(0)	1.201(0)	1.245(0)	1.312(0)	1.404(0)	1.525(0)	1.673(0)	1.848(0)
2	20	3.979(-2)	3.188(-2)	2.506(-2)	1.943(-2)	1.491(-2)	1.134(-2)	8.578(-3)	6.496(-3)
2	21	1.170(0)	1.202(0)	1.251(0)	1.322(0)	1.417(0)	1.540(0)	1.689(0)	1.863(0)
2	22	5.678(-1)	5.841(-1)	6.086(-1)	6.435(-1)	6.904(-1)	7.501(-1)	8.224(-1)	9.062(-1)
2	23	1.432(0)	1.476(0)	1.540(0)	1.629(0)	1.749(0)	1.900(0)	2.084(0)	2.298(0)
2	24	6.307(-2)	5.449(-2)	4.639(-2)	3.939(-2)	3.365(-2)	2.914(-2)	2.573(-2)	2.328(-2)
2	25	1.525(0)	1.568(0)	1.631(0)	1.722(0)	1.845(0)	2.003(0)	2.196(0)	2.421(0)
2	26	2.916(-2)	2.559(-2)	2.186(-2)	1.820(-2)	1.473(-2)	1.157(-2)	8.835(-3)	6.596(-3)
2	27	1.467(-2)	1.306(-2)	1.152(-2)	1.017(-2)	9.067(-3)	8.239(-3)	7.685(-3)	7.386(-3)
3	4	1.730(0)	1.373(0)	1.040(0)	7.658(-1)	5.582(-1)	4.091(-1)	3.057(-1)	2.355(-1)
3	5	1.403(-1)	1.111(-1)	8.433(-2)	6.275(-2)	4.668(-2)	3.530(-2)	2.753(-2)	2.235(-2)
3	6	2.742(-1)	2.101(-1)	1.574(-1)	1.172(-1)	8.769(-2)	6.677(-2)	5.229(-2)	4.251(-2)
3	7	1.733(-1)	1.256(-1)	8.864(-2)	6.187(-2)	4.343(-2)	3.122(-2)	2.343(-2)	1.865(-2)
3	8	3.235(-1)	2.474(-1)	1.870(-1)	1.424(-1)	1.113(-1)	9.053(-2)	7.726(-2)	6.930(-2)
3	9	1.388(0)	1.284(0)	1.214(0)	1.184(0)	1.192(0)	1.235(0)	1.305(0)	1.399(0)
3	10	4.489(-2)	3.279(-2)	2.335(-2)	1.636(-2)	1.135(-2)	7.813(-3)	5.343(-3)	3.625(-3)
3	11	3.332(-1)	2.965(-1)	2.706(-1)	2.560(-1)	2.516(-1)	2.557(-1)	2.666(-1)	2.826(-1)
3	12	1.261(0)	1.214(0)	1.197(0)	1.212(0)	1.259(0)	1.335(0)	1.437(0)	1.559(0)
3	13	2.353(-1)	1.853(-1)	1.460(-1)	1.164(-1)	9.463(-2)	7.882(-2)	6.763(-2)	5.996(-2)
3	14	2.668(0)	2.720(0)	2.816(0)	2.963(0)	3.166(0)	3.429(0)	3.751(0)	4.123(0)
3	15	1.146(-1)	9.239(-2)	7.521(-2)	6.251(-2)	5.354(-2)	4.756(-2)	4.396(-2)	4.223(-2)
3	16	1.634(-1)	1.411(-1)	1.249(-1)	1.145(-1)	1.090(-1)	1.078(-1)	1.100(-1)	1.151(-1)
3	17	2.010(-1)	1.687(-1)	1.430(-1)	1.244(-1)	1.123(-1)	1.058(-1)	1.039(-1)	1.057(-1)

Table 7. continued.

<i>i</i>	<i>j</i>	$\log_{10}(T[\text{K}])$							
		5.6	5.8	6.0	6.2	6.4	6.6	6.8	7.0
3	18	2.309(-1)	1.849(-1)	1.463(-1)	1.165(-1)	9.478(-2)	7.975(-2)	6.996(-2)	6.411(-2)
3	19	1.338(0)	1.360(0)	1.404(0)	1.474(0)	1.574(0)	1.704(0)	1.866(0)	2.056(0)
3	20	3.790(-1)	3.805(-1)	3.884(-1)	4.039(-1)	4.279(-1)	4.606(-1)	5.018(-1)	5.506(-1)
3	21	8.007(-2)	6.345(-2)	4.900(-2)	3.715(-2)	2.775(-2)	2.047(-2)	1.498(-2)	1.104(-2)
3	22	1.093(-2)	8.817(-3)	6.935(-3)	5.354(-3)	4.069(-3)	3.045(-3)	2.243(-3)	1.627(-3)
3	23	4.732(-2)	4.815(-1)	4.962(-1)	5.194(-1)	5.525(-1)	5.963(-1)	6.507(-1)	7.149(-1)
3	24	5.585(0)	5.750(0)	5.993(0)	6.336(0)	6.797(0)	7.387(0)	8.107(0)	8.947(0)
3	25	2.091(0)	2.149(0)	2.236(0)	2.360(0)	2.527(0)	2.742(0)	3.005(0)	3.312(0)
3	26	2.387(-1)	2.343(-1)	2.326(-1)	2.350(-1)	2.421(-1)	2.542(-1)	2.713(-1)	2.933(-1)
3	27	2.316(-2)	1.975(-2)	1.647(-2)	1.352(-2)	1.099(-2)	8.882(-3)	7.189(-3)	5.866(-3)
4	5	6.635(-1)	5.830(-1)	5.118(-1)	4.564(-1)	4.169(-1)	3.910(-1)	3.751(-1)	3.661(-1)
4	6	9.740(-2)	7.071(-2)	4.937(-2)	3.359(-2)	2.251(-2)	1.500(-2)	1.001(-2)	6.742(-3)
4	7	1.633(-1)	1.251(-1)	9.510(-2)	7.272(-2)	5.658(-2)	4.529(-2)	3.767(-2)	3.278(-2)
4	8	2.773(-1)	2.090(-1)	1.548(-1)	1.141(-1)	8.446(-2)	6.318(-2)	4.807(-2)	3.741(-2)
4	9	5.203(-1)	4.096(-1)	3.220(-1)	2.577(-1)	2.136(-1)	1.855(-1)	1.695(-1)	1.624(-1)
4	10	3.670(-2)	2.626(-2)	1.828(-2)	1.249(-2)	8.429(-3)	5.643(-3)	3.752(-3)	2.480(-3)
4	11	1.252(-1)	9.444(-2)	7.080(-2)	5.376(-2)	4.207(-2)	3.441(-2)	2.967(-2)	2.702(-2)
4	12	3.157(-1)	2.289(-1)	1.624(-1)	1.140(-1)	7.988(-2)	5.635(-2)	4.036(-2)	2.961(-2)
4	13	2.077(0)	2.012(0)	1.993(0)	2.027(0)	2.112(0)	2.244(0)	2.419(0)	2.629(0)
4	14	1.928(-1)	1.568(-1)	1.308(-1)	1.140(-1)	1.048(-1)	1.018(-1)	1.034(-1)	1.083(-1)
4	15	1.682(-1)	1.415(-1)	1.207(-1)	1.054(-1)	9.511(-2)	8.892(-2)	8.620(-2)	8.631(-2)
4	16	2.543(0)	2.590(0)	2.678(0)	2.815(0)	3.007(0)	3.254(0)	3.556(0)	3.904(0)
4	17	1.808(-1)	1.426(-1)	1.110(-1)	8.581(-2)	6.606(-2)	5.074(-2)	3.900(-2)	3.012(-2)
4	18	2.174(-1)	1.745(-1)	1.383(-1)	1.084(-1)	8.408(-2)	6.431(-2)	4.843(-2)	3.593(-2)
4	19	1.570(0)	1.585(0)	1.628(0)	1.702(0)	1.812(0)	1.957(0)	2.138(0)	2.350(0)
4	20	7.925(-2)	7.132(-2)	6.530(-2)	6.133(-2)	5.935(-2)	5.923(-2)	6.077(-2)	6.377(-2)
4	21	3.166(0)	3.234(0)	3.352(0)	3.529(0)	3.774(0)	4.091(0)	4.478(0)	4.929(0)
4	22	1.383(-2)	1.150(-2)	9.393(-3)	7.534(-3)	5.923(-3)	4.548(-3)	3.401(-3)	2.476(-3)
4	23	9.660(-2)	8.884(-2)	8.339(-2)	8.034(-2)	7.965(-2)	8.122(-2)	8.489(-2)	9.043(-2)
4	24	2.966(-1)	2.841(-1)	2.778(-1)	2.780(-1)	2.848(-1)	2.984(-1)	3.187(-1)	3.450(-1)
4	25	4.631(-1)	4.607(-1)	4.659(-1)	4.801(-1)	5.044(-1)	5.396(-1)	5.855(-1)	6.413(-1)
4	26	5.240(0)	5.377(0)	5.588(0)	5.896(0)	6.316(0)	6.861(0)	7.531(0)	8.314(0)
4	27	7.081(-2)	6.353(-2)	5.702(-2)	5.205(-2)	4.882(-2)	4.720(-2)	4.688(-2)	4.750(-2)
5	6	1.464(-2)	1.059(-2)	7.334(-3)	4.922(-3)	3.234(-3)	2.095(-3)	1.344(-3)	8.576(-4)
5	7	2.641(-2)	1.946(-2)	1.412(-2)	1.030(-2)	7.714(-3)	6.049(-3)	5.038(-3)	4.473(-3)
5	8	3.787(-2)	2.684(-2)	1.842(-2)	1.235(-2)	8.144(-3)	5.312(-3)	3.438(-3)	2.213(-3)
5	9	5.249(-2)	3.688(-2)	2.511(-2)	1.672(-2)	1.097(-2)	7.129(-3)	4.606(-3)	2.970(-3)
5	10	1.419(-2)	1.162(-2)	9.376(-3)	7.480(-3)	5.885(-3)	4.542(-3)	3.424(-3)	2.517(-3)
5	11	5.438(-2)	4.568(-2)	3.833(-2)	3.249(-2)	2.803(-2)	2.478(-2)	2.257(-2)	2.123(-2)
5	12	6.549(-2)	5.113(-2)	3.954(-2)	3.039(-2)	2.318(-2)	1.745(-2)	1.291(-2)	9.349(-3)
5	13	1.101(-1)	7.947(-2)	5.568(-2)	3.820(-2)	2.586(-2)	1.736(-2)	1.158(-2)	7.696(-3)
5	14	1.020(-1)	9.237(-2)	8.619(-2)	8.345(-2)	8.387(-2)	8.702(-2)	9.242(-2)	9.960(-2)
5	15	2.378(-2)	1.839(-2)	1.385(-2)	1.025(-2)	7.478(-3)	5.387(-3)	3.827(-3)	2.677(-3)
5	16	6.586(-1)	6.525(-1)	6.601(-1)	6.825(-1)	7.200(-1)	7.722(-1)	8.378(-1)	9.148(-1)
5	17	3.358(-2)	2.665(-2)	2.058(-2)	1.562(-2)	1.171(-2)	8.674(-3)	6.353(-3)	4.600(-3)
5	18	3.335(-2)	2.756(-2)	2.242(-2)	1.797(-2)	1.414(-2)	1.088(-2)	8.157(-3)	5.955(-3)
5	19	4.243(-2)	3.179(-2)	2.317(-2)	1.659(-2)	1.176(-2)	8.298(-3)	5.833(-3)	4.086(-3)
5	20	2.862(-2)	2.274(-2)	1.782(-2)	1.404(-2)	1.130(-2)	9.444(-3)	8.291(-3)	7.675(-3)
5	21	5.248(-2)	3.906(-2)	2.835(-2)	2.026(-2)	1.436(-2)	1.015(-2)	7.169(-3)	5.059(-3)
5	22	5.403(-3)	4.357(-3)	3.463(-3)	2.715(-3)	2.095(-3)	1.585(-3)	1.172(-3)	8.462(-4)
5	23	2.403(-2)	1.803(-2)	1.340(-2)	9.951(-3)	7.459(-3)	5.699(-3)	4.486(-3)	3.675(-3)
5	24	1.556(-2)	1.180(-2)	8.799(-3)	6.461(-3)	4.672(-3)	3.322(-3)	2.320(-3)	1.594(-3)
5	25	2.464(-2)	1.867(-2)	1.382(-2)	1.005(-2)	7.207(-3)	5.101(-3)	3.560(-3)	2.449(-3)
5	26	4.375(-2)	3.737(-2)	3.258(-2)	2.933(-2)	2.743(-2)	2.661(-2)	2.663(-2)	2.721(-2)
5	27	2.179(0)	2.247(0)	2.347(0)	2.485(0)	2.670(0)	2.905(0)	3.190(0)	3.521(0)

Notes. The indices (*j*, *i*) correspond to the levels as shown in Table 5. ^(†) In this table, 5.324(-1) denotes 5.324×10^{-1} .

systematically lower than their own values at higher temperatures, which they attribute to the calculation of Gupta & Tayal (1998) only extending to 60 Ryd. In Fig. 7 we compare our results with those of Gupta & Tayal (1998) at 5×10^6 K for strong optically allowed transitions. This figure indeed shows that the

results of Gupta & Tayal (1998) are systematically lower at this temperature for this set of transitions. If, however, we compare results for transitions which do not satisfy the rigorous electric dipole selection rules also at 5×10^6 K (Fig. 8), we find good agreement, now with the exception of transition 1-5.

Table 8. Transition probabilities (A_{ji} , units s^{-1}) calculated with the target (Table 4).

j	i	A_{ji}												
2	1	1.396(1)	8	3	5.131(7)	14	3	3.348(10)	18	12	2.082(1)	23	3	1.269(10)
3	1	6.369(-3)	8	4	1.084(7)	14	4	6.486(8)	18	13	2.204(-1)	23	4	1.420(9)
3	2	9.753(0)	9	3	1.330(9)	14	5	4.137(8)	18	15	1.591(-4)	23	5	1.183(7)
4	1	3.099(-3)	9	4	9.857(7)	15	2	1.168(8)	18	17	1.907(1)	24	3	6.461(10)
4	2	6.976(1)	10	2	4.342(9)	15	3	1.532(8)	19	2	1.789(10)	24	4	2.405(9)
4	3	8.414(1)	11	1	1.309(9)	15	4	3.534(8)	19	3	1.808(10)	25	2	2.384(10)
5	2	1.062(3)	11	2	1.993(9)	16	1	9.499(8)	19	4	1.589(10)	25	3	3.364(10)
5	3	4.360(0)	11	3	9.593(8)	16	2	5.280(9)	20	1	4.614(10)	25	4	6.628(9)
5	4	7.614(0)	11	4	5.629(7)	16	3	1.078(9)	20	2	2.667(8)	26	3	3.427(9)
6	2	5.394(6)	11	5	2.285(7)	16	4	2.967(10)	20	3	7.082(9)	26	4	6.852(10)
6	3	8.800(6)	12	2	4.430(8)	16	5	4.243(9)	20	4	7.986(8)	27	1	3.527(8)
6	4	2.370(5)	12	3	3.458(9)	17	3	3.358(8)	20	5	5.201(7)	27	2	1.481(8)
7	1	1.365(9)	12	4	5.306(6)	17	4	2.161(7)	21	2	2.039(10)	27	3	5.872(4)
7	2	3.551(8)	13	2	7.750(7)	18	3	2.598(1)	21	3	8.821(7)	27	4	1.235(8)
7	3	1.306(7)	13	3	1.042(8)	18	4	2.256(1)	21	4	3.649(10)	27	5	5.636(10)
7	4	2.885(7)	13	4	5.464(9)	18	6	4.352(0)	22	2	4.659(10)	0	0	0.000(0)
7	5	2.677(6)	14	1	6.878(9)	18	8	1.111(1)	23	1	8.189(9)	0	0	0.000(0)
8	2	1.562(9)	14	2	1.705(10)	18	9	1.424(1)	23	2	4.047(10)	0	0	0.000(0)

Notes. The indices (j, i) correspond to the levels as shown in Table 5.

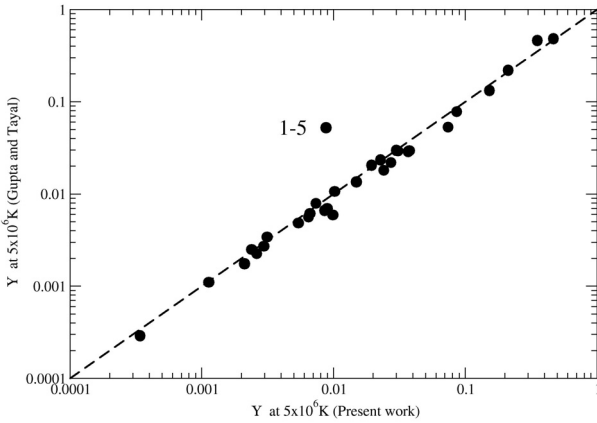


Fig. 8. Comparison of thermally averaged collision strengths at 5×10^6 K from the present work and from Gupta & Tayal (1998). Transitions are included between the three energetically lowest levels and all levels of the $3s3p^3$ and $3s^23p3d$ configurations which do not satisfy the rigorous electric dipole selection rule between LSJ levels.

Thus at the higher temperatures, the thermally averaged collision strengths of Gupta & Tayal (1998) are systematically lower than the present work but only for the strong electric dipole allowed transitions. This picture is consistent with the reason put forward by Aggarwal & Keenan (2005) since the collision strengths for the allowed transitions are increasing with energy and therefore particularly sensitive to the absence of data beyond 60 Ryd.

The discrepancy for the 1–5 transition ($3s^23p^2\ ^3P_0 - 3s^23p^2\ ^1S_0$), has also been noted by Aggarwal & Keenan (2005) as being due to an earlier bug in the R -matrix code which caused the collision strengths between $J = 0$ states of the same parity to be overestimated.

Aggarwal & Keenan (2005) also draw attention to the increasingly large differences in thermally averaged collision strengths between their work and that of Gupta & Tayal (1998) as the electron temperature is reduced. In Fig. 9 we compare our results with those of both Aggarwal & Keenan (2005) and Gupta & Tayal (1998) for the transitions among the levels of the lowest $3s^23p^3$ configuration at 10^5 K. The differences between all

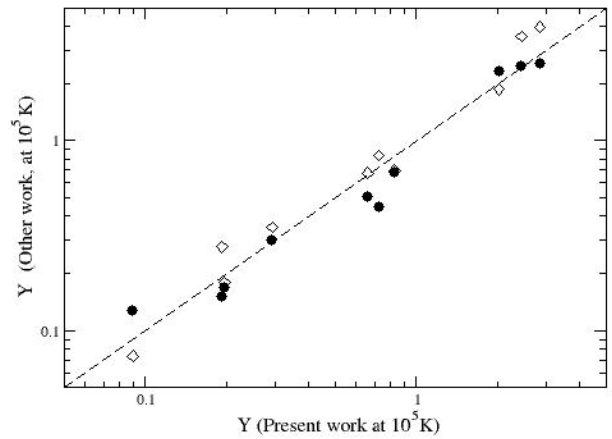


Fig. 9. Comparison of thermally averaged collision strengths at 10^5 K from the present work and from Gupta & Tayal (1998) (filled circles) and Aggarwal & Keenan (2004) (open diamonds). Transitions are included between the five energetically lowest levels.

three calculations are significantly larger than those found at the higher temperatures but no clear picture emerges. The average absolute percentage difference between our results and those of Gupta & Tayal (1998) is 19% while for Aggarwal & Keenan (2004) it is 21%. The maximum differences are 43% and 44% respectively. The lower the temperature, the more the thermally averaged collision strengths depend on a few near threshold resonances, the uncertainty in the positions of which becomes increasingly important. It is our view that the scatter in the results at 10^5 K is a measure of the real uncertainty in the published low temperature results at present. Further work is needed to examine the convergence of the low temperature thermally averaged collision strengths as target size is increased.

Tables of the thermally averaged collision strengths for all 114 levels will be made available in electronic form at the Centre de Données astronomiques de Strasbourg (CDS). The results deposited at the CDS will also include a full set of radiative transition probabilities. In Table 8, we give the radiative transition probabilities for the 27 levels of the three energetically lowest configurations as calculated in the 72CF calculation with

TECs and using experimental energies. Transition probabilities are not included if they constitute less than 0.01% of the total radiative probability from a given upper level. The full set of results, plus the energy resolved collision strengths will also be available from the database TIPbase. We refer readers to the database website (<http://cdsweb.u-strasbg.fr/tipbase/home.html>) for further information.

4. Summary and conclusions

A new calculation of collision strengths and rates for electron collisional excitation of Fe XIII has been described.

We find very good agreement with the thermally averaged collision strengths of [Gupta & Tayal \(1998\)](#) at temperatures at which Fe¹²⁺ has its maximum abundance in the solar corona. There is, however, clear evidence that their thermally averaged collision strengths are underestimated at the higher temperatures for strong dipole allowed transitions.

Comparison of the present results with those of [Aggarwal & Keenan \(2004, 2005\)](#) show significant differences for several important optically allowed transitions. These discrepancies are not due to their use of a fully relativistic treatment but rather to their restricted configuration basis.

On the other hand, the present results for the forbidden transitions within the ground electron configuration at a temperature of 10⁵ K show significant differences to both those of [Aggarwal & Keenan \(2005, 2004\)](#) and [Gupta & Tayal \(1998\)](#). We conclude that these differences must be taken as a measure in the uncertainty in all the calculated results at the lower temperatures, where the exact position and magnitude of near threshold resonances become increasingly important.

Acknowledgements. Support from STFC is acknowledged. P.J.S. would also like to acknowledge the support of the Université Paris 7 “Denis Diderot” and the hospitality of the Observatoire de Paris. We thank Dr. Giulio del Zanna for many useful discussions and Dr. H. E. Mason for a critical reading of the manuscript.

References

- Aggarwal, K. M., & Keenan, F. P. 2004, A&A, 418, 371
 Aggarwal, K. M., & Keenan, F. P. 2005, A&A, 429, 1117
 Bryans, P., Badnell, N. R., Gorczyca, T. W., et al. 2006, ApJS, 167, 245
 Burgess, A. 1974, JPhB, 7, L364
 Burgess, A., & Tully, J. A. 1992, A&A, 254, 436
 Czyzak, S. J., Krueger, T. K., Saraph, H. E., & Shemming, J. 1967, Proc. Phys. Soc., 92, 1146
 Dylla, K. G., Grant, I. P., Johnson, C. T., Parpia, F. A., & Plummer, E. P. 1989, CoPhC, 55, 424
 Eissner, W., Jones, M., & Nussbaumer, H. 1974, CoPhC, 8, 270
 Fawcett, B. C., & Mason, H. E. 1989, ADNDT, 43, 245
 Flower, D. R. 1971, JPhB, 4, 697
 Flower, D. R., & Nussbaumer, H. 1974, A&A, 31, 353
 Griffin, D. C., Badnell, N. R., & Pindzola, M. S. 1998, JPhB, 31, 3713
 Gupta, G. P., & Tayal, S. S. 1998, ApJ, 506, 464
 Hibbert, A. 1975, CoPhC, 9, 141
 Hummer, D. G., Berrington, K. A., Eissner, W., et al. 1993, A&A, 279, 298
 Jupen, C., Isler, R. C., & Trabert, E. 1993, MNRAS, 264, 627
 Keenan, F. P., Foster, V. J., Drake, J. J., Tayal, S. S., & Widing, K. G. 1995, ApJ, 453, 906
 Landi, E. 2002, A&A, 382, 1106
 Martin, W. C., et al. 1995, NIST Database for Atomic Spectroscopy, Version 3.0, NIST Standard Reference Database 61
 Nussbaumer, H., & Storey, P. J. 1978, A&A, 64, 139
 Penn, M. J., & Kuhn, J. R. 1994, ApJ, 434, 807
 Storey, P. J., Mason, H. E., & Young, P. R. 2000, A&AS, 141, 285
 Tayal, S. S. 1995, ApJ, 446, 895
 Tayal, S. S. 2000, ApJ, 544, 575
 Young, P. R. 2004, A&A, 417, 785
 Zeippen, C. J., Seaton, M. J., & Morton, D. C. 1977, MNRAS, 181, 527